



Mushroom vortex street

Meng Shi ^{1,2,*} and Sigurdur T. Thoroddsen ^{2,†}¹*School of Mechanical Engineering, Xi'an Jiaotong University, Xi'an 710049, People's Republic of China*²*High-Speed Fluids Imaging Laboratory, Physical Science and Engineering Division, King Abdullah University of Science and Technology (KAUST), Thuwal 23955-6900, Saudi Arabia*

(Received 15 June 2023; published 20 November 2023)

This paper is associated with a poster winner of a 2022 American Physical Society's Division of Fluid Dynamics (DFD) Milton van Dyke Award for work presented at the DFD Gallery of Fluid Motion. The original poster is available online at the Gallery of Fluid Motion, <https://doi.org/10.1103/APS.DFD.2022.GFM.P0039>

DOI: [10.1103/PhysRevFluids.8.110512](https://doi.org/10.1103/PhysRevFluids.8.110512)

Marangoni-driven flows arise from spatial variations of surface tension along a free surface, which usually occurs where temperature or concentration gradients are present [1,2]. The unbalanced stress tangent along the free surface also promotes motions inside the bulk liquid. This occurs when stirring together different miscible liquids or by uneven heating of liquid in a container. These situations occur frequently during processing in the chemical, beverage, and food industries [3]. Other Marangoni-induced phenomena are common in daily life, such as coffee rings [4,5], tears of wine [6–8], and inkjet printing [9], can cause enhanced splashing [10] and flow patterns in soap bubbles [11]. These motions often produce intricate patterns on the free surface. One striking example emerges following the impact of a drop on a miscible pool of a different liquid [12,13]. In the immiscible case a drop of oil will spread on water to form a molecular-thin film. This can also lead to “Marangoni bursting,” when the drop is highly volatile and the edge of the spreading film fragments and releases a regular stream of minute droplets [14]. On the other hand, when a miscible drop with lower surface tension is deposited on a pool surface with stronger surface tension, its edge is pulled outwards to spread and mix with the underlying pool. This motion will continue until the surface-tension difference is neutralized. This spreading can generate a characteristic vortex ring under the edge of the spreading disk [15–17]. For the inverted problem, with the drop liquid having the stronger surface tension, a Marangoni-driven vortex ring appears inside the drop [12]. On the time scale of a minute, this motion forms a flowerlike pattern [13]. Herein, we use high-speed video imaging to discover a related Marangoni-driven instability in the same configuration, but one that appears within the first few milliseconds, i.e., a row of mushroomlike vortices aligning in a regular pattern in the azimuthal direction, as shown in the accompanying figures. These early rapidly rotating vortices were entirely missed in the earlier snapshots of this impact configuration [12].

Our experimental configuration is a water drop impacting on a thin layer of glycerin. Figure 1 shows the experimental setup and resulting morphology, where the drop spreads impulsively and splits into two parts, an outer ring and an inner circular disk. We observe this formation with two

*mengshi@xjtu.edu.cn

†sigurdur.thoroddsen@kaust.edu.sa

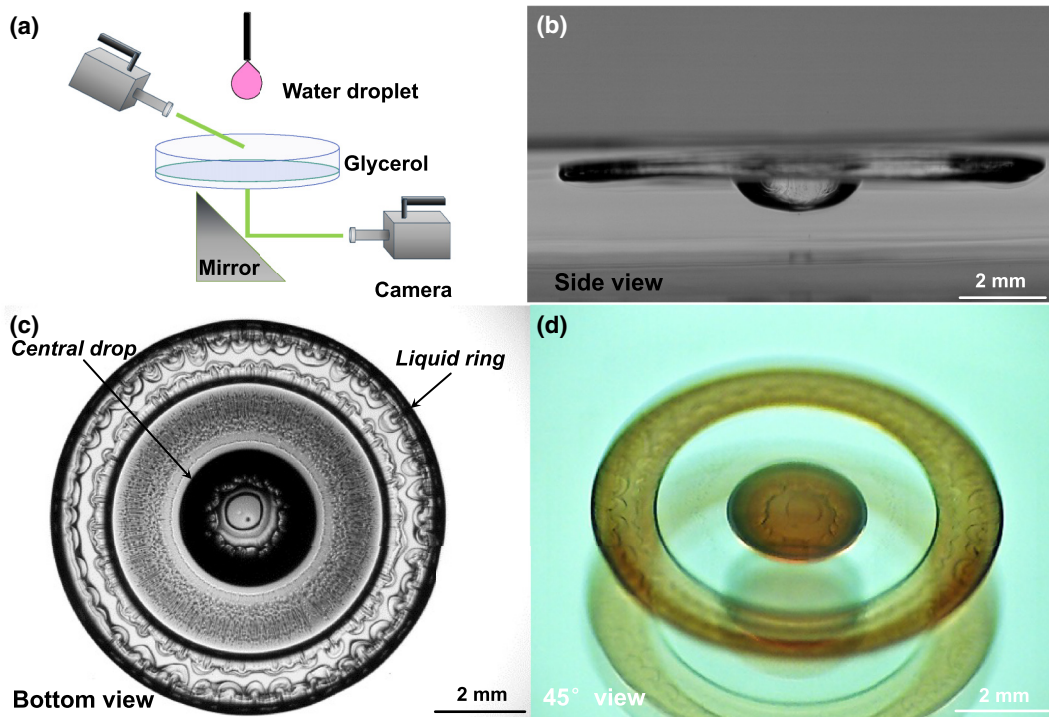


FIG. 1. Central disk and ring configuration resulting from the impact of a $D = 3$ mm water drop onto a 1.5-mm-deep glycerol film, shown through three different views. The experimental setup is shown in (a). The frame in (b) is shown ~ 178 ms after impact and the frames in (c) and (d) are shown ~ 96 ms after impact. The impact velocity is $U = 2.89$ m/s and the corresponding $Re = 8670$ and $We = 343$. The Marangoni number is $Ma = 7.78 \times 10^4$ and characterizes the driving force along the free surface, as defined in Eq. (2).

synchronized high-speed video cameras, one (Phantom V2511) viewing from the bottom, through a glass plate, with the second one (color Photron SA3) from the top at a 45° angle [Fig. 1(a)]. Coloring the drop liquid (5 g/L strawberry red dye, Bin Afif) shows clearly the splitting of the drop into two. The separate sideview in Fig. 1(b) shows that the central disk is much deeper than the outer ring, owing to the original impact energy and vertical momentum, which is sufficient to deform the much-more-viscous glycerin film. The impact lamella spreads along the glycerin with a thicker edge. The thinner region away from this edge then dewets, forming intriguing radial interconnected tendrils, visible in Fig. 1(c) and in the close-up image at the inner edge of the ring in Fig. 2. To characterize the relative strength of the impact inertia vs viscous and vs surface tension, respectively, we use the Reynolds and Weber numbers of the impact, defined as

$$Re = \frac{\rho_w U D}{\mu_w}, \quad We = \frac{\rho_w U^2 D}{\sigma_w}, \quad (1)$$

where the properties of the water are used for dynamic viscosity $\mu_w \simeq 10^{-3}$ Pa s, density ρ_w , and surface tension σ_w .

The impact generates fresh contact lines between the water and glycerin—first at the outer edge of the ring, where Marangoni forces produce spontaneous radial motions at the free surface. The surface tension of the water is $\sigma_w = 73$ mN/m vs $\sigma_g = 65$ mN/m for the glycerin, so $\Delta\sigma = \sigma_w - \sigma_g = 8$ mN/m drives the motions towards the water, forming counter-rotating vortices within the water ring and one vortex ring within the central disk. These vortices are initially axisymmetric,

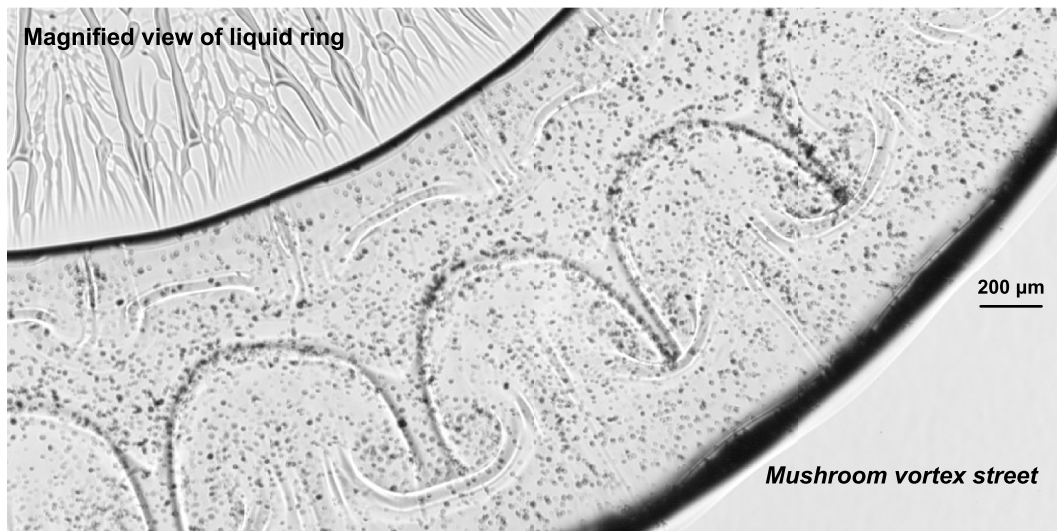


FIG. 2. Close-up of the azimuthal mushroom vortex street, for the same conditions as in the earlier figure. The black dots are silver-coated hollow particles ($\sim 10 \mu\text{m}$). The video frame is taken at 75 ms after the drop impact. The top left corner shows the tendrils of water left on the glycerin surface after the rupture of the thin water layer of the spreading lamella.

but the progenitors of the azimuthal mushroom vortices are visible after only 50 ms. The index of refraction difference, between the two liquids, reveals these regular vortices inside the outer ring, in Fig. 1(c). The large bottom curvature in the central water disk diffracts the illuminating light and hides those vortices in the bottom view. The vortices appear on both sides of the ring with the outer edge having wavelength of $\lambda_\theta \simeq 800 \mu\text{m}$, while being somewhat smaller on the inner side of the ring. This proves that the appearance of mushroom vortices is independent on the in-plane curvature of the water-glycerin interface (the curved dark lines in Fig. 2).

To study the dynamics underlying this instability, we seed the water with small neutrally buoyant particles (Dantec, S-HGS-10, $10 \mu\text{m}$ diameter) and use a long-distance microscope (Leica Z16 APO), with adjustable magnification and aperture, to gain a pixel resolution as fine as $2 \mu\text{m}/\text{px}$. We use frame rates up to 10 000 fps and frame exposure of $30 \mu\text{s}$ to eliminate smearing of the particle images. The particles near the free surface are pulled towards the water at the highest speed of $u_p \simeq 0.5 \text{ m/s}$. This speed is similar to the largest velocities observed for the oil drop spreading on pool surface configuration by Li *et al.* [17]. They match the surface Marangoni stress to the viscous stress under the surface film, i.e., $\Delta\sigma/W = \mu_w u_p/\delta$. In our study $W \sim 970 \mu\text{m}$ is the half width of the water ring in the radial direction and $\delta \sim 100 \mu\text{m}$ is half its depth. This gives $u_p = \Delta\sigma \delta/(\mu_w W) \sim 0.8 \text{ m/s}$, of the same order as observed. In our configuration the viscous stress can be expected to be larger, i.e., the small amount of glycerin pulled along the water surface has about 10^3 higher viscosity than the water, and thereby, as the two liquids mix, the mixture has higher viscosity. One can also imagine a thin layer of glycerin being pulled along the water layer, making extensional film viscosity become relevant. The strength of the driving force is characterized by the Marangoni number, which has two different length scales: one the thickness of the water layer δ and the half width W of the ring, i.e.,

$$\text{Ma} = \frac{\Delta\sigma \delta^2}{\mu_w \alpha W} \simeq 7.78 \times 10^4, \quad (2)$$

where $\alpha \sim 1.06 \times 10^{-9} \text{ m}^2/\text{s}$ is the diffusivity of glycerin into the water.

These robust vortices persist for about $T_\alpha \simeq 350$ ms and then abruptly slow down. This occurs when there has been sufficient mixing of glycerin into the water to significantly reduce $\Delta\sigma$. Thereafter, much slower motions where Marangoni effects are influenced by diffusion and rebounding by gravity lead to the flower formation. These order-of-magnitude slower velocities correspond well with values observed in [12] using a regular video camera. The time scale of the intense mixing can be estimated from the stirring and diffusion of tendrils of glycerin, visible in some of the side views, which are wrapped around the Marangoni-driven vortex inside the water ring. Taking into account the much slower return velocity below the water surface, the wrapping of the glycerin tendril should take about $T_w \sim 2W/(0.1 \times u_p) \sim 38$ ms, thereby giving enough time for nearly nine windings during diffusion time T_α . The glycerin tendril would therefore be $L_g \sim 9 \times 2 \times W \simeq 18$ mm long. Furthermore, by assuming an average diffusive thickness of this tendril to be $\delta_g \sim \sqrt{\alpha T_\alpha/2} \sim 14$ μm , the area of mixed glycerin becomes 0.25 mm^2 , if one takes into account both sides of the thread. This is of similar size as the cross-sectional area of the water disk $2\delta W \simeq 0.19$ mm^2 , justifying the proposed neutralization of the Marangoni stress, after mixing time of T_α .

Besides the aesthetic beauty of these instabilities, our confined geometry presents an ideal test bed for the onset and transient dynamics of Marangoni-driven flows.

This work was financially supported by King Abdullah University of Science and Technology (KAUST) under Grant No. BAS/1/1352-01-01.

-
- [1] L. Scriven and C. Sternling, The Marangoni effects, *Nature (London)* **187**, 186 (1960).
 - [2] P.-G. De Gennes, F. Brochard-Wyart, and D. Quéré, *Capillarity and Wetting Phenomena: Drops, Bubbles, Pearls, Waves* (Springer, Berlin, 2004).
 - [3] D. L. Pyle, P. J. Fryer, and C. D. Reilly, *Chemical Engineering for the Food Industry* (Springer Science and Business Media, New York, 2012).
 - [4] R. D. Deegan, O. Bakajin, T. F. Dupont, G. Huber, S. R. Nagel, and T. A. Witten, Capillary flow as the cause of ring stains from dried liquid drops, *Nature (London)* **389**, 827 (1997).
 - [5] P. J. Yunker, T. Still, M. A. Lohr, and A. Yodh, Suppression of the coffee-ring effect by shape-dependent capillary interactions, *Nature (London)* **476**, 308 (2011).
 - [6] J. Fournier and A. Cazabat, Tears of wine, *Europhys. Lett.* **20**, 517 (1992).
 - [7] A. E. Hosoi and J. W. Bush, Evaporative instabilities in climbing films, *J. Fluid Mech.* **442**, 217 (2001).
 - [8] D. C. Venerus and D. N. Simavilla, Tears of wine: New insights on an old phenomenon, *Sci. Rep.* **5**, 16162 (2015).
 - [9] D. Soltman and V. Subramanian, Inkjet-printed line morphologies and temperature control of the coffee ring effect, *Langmuir* **24**, 2224 (2008).
 - [10] A. B. Aljedaani, C. Wang, A. Jetly, and S. T. Thoroddsen, Experiments on the breakup of drop-impact crowns by marangoni holes, *J. Fluid Mech.* **844**, 162 (2018).
 - [11] S. F. Ahmadi, S. Nath, C. M. Kingett, P. Yue, and J. B. Boreyko, How soap bubbles freeze, *Nat. Commun.* **10**, 2531 (2019).
 - [12] E. Tan and S. Thoroddsen, Marangoni instability of two liquids mixing at a free surface, *Phys. Fluids* **10**, 3038 (1998).
 - [13] E. Tan and S. Thoroddsen, The thistle crown, *Phys. Fluids* **10**, S7 (1998).
 - [14] L. Keiser, H. Bense, P. Colinet, J. Bico, and E. Reyssat, Marangoni bursting: Evaporation-induced emulsification of binary mixtures on a liquid layer, *Phys. Rev. Lett.* **118**, 074504 (2017).
 - [15] A. D. Dussaud and S. M. Troian, Dynamics of spontaneous spreading with evaporation on a deep fluid layer, *Phys. Fluids* **10**, 23 (1998).

- [16] H. Kim, K. Muller, O. Shardt, S. Afkhami, and H. A. Stone, Solutal Marangoni flows of miscible liquids drive transport without surface contamination, [Nat. Phys. **13**, 1105 \(2017\)](#).
- [17] Y. Li, A. A. Pahlavan, Y. Chen, S. Liu, Y. Li, H. A. Stone, and S. Granick, Oil-on-water droplets faceted and stabilized by vortex halos in the subphase, [Proc. Natl. Acad. Sci. USA **120**, e2214657120 \(2023\)](#).